Grayscale photomask fabricated by laser direct writing in metallic nano-films

Chuan Fei Guo,[1,2] Sihai Cao,[1,2] Peng Jiang,[1] Ying Fang,[1] Jianming Zhang,[1,2] Yongtao Fan,[1,3] Yongsheng Wang,[1,2] Wendong Xu,[1,3] Zhensheng Zhao,[4] and Qian Liu[1,*]

[1]*National Center for Nanoscience and Technology, China, No. 11Beiyitiao, Zhongguancun, Beijing100190, China*
[2]*Graudate School of the Chinese Academy of Sciences, Beijing100080, China*
[3]*Shanghai Institute of Optics and Fine Mechanics, Chinese Academy of Sciences, No. 390, Qinghe Road, Shanghai 201800, China*
[4]*Technical Institute of Physics & Chemistry, Chinese Academy of Sciences, No. 2 Zhongguancun, Beijing 100190, China*
*liuq@nanoctr.cn

Abstract: The grayscale photomask plays a key role in grayscale lithography for creating 3D microstructures like micro-optical elements and MEMS structures, but how to fabricate grayscale masks in a cost-effective way is still a big challenge. Here we present novel low cost grayscale masks created in a two-step method by laser direct writing on Sn nano-films, which demonstrate continuous-tone gray levels depended on writing powers. The mechanism of the gray levels is due to the coexistence of the metal and the oxides formed in a laser-induced thermal process. The photomasks reveal good technical properties in fabricating 3D microstructures for practical applications.

OCIS codes: (160.4236) Nanomaterials; (310.6845) Thin film devices and applications; (110.6895) Three-dimensional lithography; (160.3900) Metals.

References and links

1. J. D. Rogers, A. H. O. Kärkkäinen, T. Tkaczyk, J. T. Rantala, and M. R. Descour, "Realization of refractive microoptics through grayscale lithographic patterning of photosensitive hybrid glass," Opt. Express **12**(7), 1294–1303 (2004), http://www.osa-jon.org/viewmedia.cfm?id=79451&seq=0.
2. K. Reimer, H. J. Quenzer, M. Jürss, and B. Wagner, "Micro-optic fabrication using one-level gray-tone lithography," Proc. SPIE **3008**, 279–288 (1997), http://www.mp-cc.de/docs/reiphot.pdf.
3. H. Jiang, X. Yuan, Z. Yun, Y. C. Chan, and Y. L. Lam, "Fabrication of microlens in photosensitive hybrid sol–gel films using a gray scale mask," Mater. Sci. Eng. C **99**, 16 (2001).
4. M. Christophersen, and B. F. Phlips, "Gray-tone lithography using an optical diffuser and a contact aligner," Appl. Phys. Lett. **92**(19), 194102 (2008).
5. C. Gimkiewicz, D. Hagedorn, J. Jahns, E.-B. Kley, and F. Thoma, "Fabrication of microprisms for planar optical interconnections by use of analog gray-scale lithography with high-energy-beam-sensitive glass," Appl. Opt. **38**(14), 2986–2990 (1999).
6. C. M. Waits, B. Morgan, M. Kastantin, and R. Ghodssi, "Microfabrication of 3D silicon MEMS structures using gray-scale lithography and deep reactive ion etching," Sens. Actuators A Phys. **119**(1), 245–253 (2005).
7. C. M. Waits, A. Modafe, and R. Ghodssi, "Investigation of gray-scale technology for large area 3D silicon MEMS structures," J. Micromech. Microeng. **13**(2), 170–177 (2003).
8. G. Gal, "Method for fabricating microlenses," U.S. Patent No. 5,310,623, 10, (1994).
9. C. K. Wu, "Method of making high energy beam sensitive glasses," U.S. Patent, No. 5,078,771 (1992).
10. C. Chen, D. Hirdes, and A. Folch, "Gray-scale photolithography using microfluidic photomasks," Proc. Natl. Acad. Sci. U.S.A. **100**(4), 1499–1504 (2003), http://www.pnas.org/cgi/content/full/100/4/1499.
11. Z. L. Wang, and Z. Pan, "Junctions and networks of SnO nanoribbons," Adv. Mater. **14**(15), 1029–1032 (2002), http://www.nanoscience.gatech.edu/zlwang/paper/2002/02_AM_2.pdf.
12. Z. W. Pan, Z. R. Dai, and Z. L. Wang, "Nanobelts of semiconducting oxides," Science **291**(5510), 1947–1949 (2001).
13. A. F. Lee, and R. M. Lambert, "Oxidation of Sn overlayers and the structure and stability of Sn oxide films on Pd (111)," Phys. Rev. B **58**(7), 4156–4165 (1998).
14. X. Q. Pan, and L. Fu, "Oxidation and phase transitions of epitaxial tin oxide thin films on (10-12) sapphire," J. Appl. Phys. **89**(11), 6048 (2001).
15. J. Arbiol, E. Comini, G. Faglia, G. Sberveglieri, and J. R. Morante, "Orthorhombic Pbcn SnO_2 nanowires for gas sensing applications," J. Cryst. Growth **310**(1), 253–260 (2008).

#117173 - $15.00 USD Received 18 Sep 2009; revised 10 Oct 2009; accepted 10 Oct 2009; published 19 Oct 2009

16. Y. X. Chen, L. J. Campbell, and W. L. Zhou, "Self-catalytic branch growth of SnO_2 nanowire junctions," J. Cryst. Growth **270**(3-4), 505–510 (2004).
17. A. Kolmakov, Y. Zhang, and M. Moskovits, "Topotactic thermal oxidation of Sn nanowires: Intermediate suboxides and core-shell metastable structures," Nano Lett. **3**(8), 1125–1129 (2003).
18. M. Batzill, and U. Diebold, "The surface and materials science of tin oxide," Prog. Surf. Sci. **79**(2-4), 47–154 (2005), http://shell.cas.usf.edu/~mbatzill/papers/paper%207.pdf.
19. E. P. Domashevskaya, O. A. Chuvenkova, V. M. Kashkarov, S. B. Kushev, S. V. Ryabtsev, S. Yu. Turishchev, and Yu. A. Yurakov, "TEM and XANES investigations and optical properties of SnO nanolayers," Surf. Interface Anal. **38**(4), 514–517 (2006).
20. C. F. Guo, Z. Zhang, S. Cao, and Q. Liu, "Laser direct writing of nanoreliefs in Sn nanofilms," Opt. Lett. **34**(18), 2820–2822 (2009).
21. J. Zhao, L. H. Huo, S. Gao, H. Zhao, and J. G. Zhao, "Alcohols and acetone sensing properties of SnO_2 thin films deposited by dip-coating," Sens. Actuators B Chem. **115**(1), 460–464 (2006).
22. F. J. Lamelas, and S. A. Reid, "Thin-film synthesis of the orthorhombic phase of SnO_2," Phys. Rev. B **60**(13), 9347–9352 (1999).

1. Introduction

The modern fast-changing telecommunication, computer, information display and imaging technologies create increasing demands for the integration of electronic and photonic systems. The miniaturization of optical devices has been an essential task before us. High efficiency micro-optical devices are commonly fabricated by grayscale lithography in combination with reactive ion etching (RIE) [1–5]. This technique is also suitable for fabricating three dimension (3D) micro-electromechanical system (MEMS) structures [6,7]. Usually, the grayscale masks are made by (1) adjusting the subresolution opening densities and/or sizes in a chromium film on glass (COG) [2,8], or (2) using high-energy-beam-sensitive (HEBS) glass [9]. In the mask fabricating process, although the former adopts a very simple material (Cr film on glass), it needs many steps like film deposition, lithography, etching, resist striping *etc.*; while the latter, shows its disadvantages for very complicated material system as well as its dependence on the expensive electron beam system, but its simple two-step mask-fabricating process (glass making and electron-beam direct writing) is attractive. Both techniques are often too costly for industrial applications. Generally speaking, an excellent grayscale mask should satisfy the following requirements: (a) continuous-tone gray levels; (b) high resolution; (c) simple techniques; (d) simple and low cost material system and (e) good photothermal stability.

In order to meet the above requirements, novel grayscale masks based on the simple and cost-effective metallic Sn films has been explored, which are entirely different from the previous efforts [8–10]. In principle, metals are opaque and many of them can be transformed into transparent metallic oxides by laser irradiation on the metallic films. And we have found continuously variable transmittance (*T*) is available for some system consisting of a metal and its oxides, for example, the system of Sn and tin oxides. Therefore, a metal/oxides system-based grayscale mask can be created by only two simple steps: metallic film deposition and laser direct writing (LDW). The Sn/tin oxides system is a very appropriate candidate for this purpose. There are three relatively stable tin oxides, tetragonal (t-) SnO, orthorhombic (o-) SnO_2 and t-SnO_2 [11–19]. Among of them, t-SnO_2 is the most transparent, followed by o-SnO_2. The t-SnO is undesired for many applications such as transparent conducting films due to its adverse impact onto transparency, but this characteristic is helpful to grayscale masks because it may bring better gray levels. Besides these oxides, we have reported another transparent and stable phase: amorphous SnO_x [20]. The different optical properties of Sn and tin oxides provide the possibility to adjust the transparency of the films because of controllable phase compositions at various temperatures so that it might be used as a potential grayscale material. Moreover, the Sn and tin oxides system has an applicable wavelength range in the visible and near ultraviolet region down to 350 nm, since SnO_2 is very transparent in the region [21].

In this study, we report on a method, in which the cost-effective grayscale masks can be fabricated simply by using laser direct writing (LDW) on the metallic Sn thin films. The mechanism of the grayscale feature of the mask is proposed based on analyzing its crystal

#117173 - $15.00 USD Received 18 Sep 2009; revised 10 Oct 2009; accepted 10 Oct 2009; published 19 Oct 2009

structure evolution as well as changes of optical properties. In addition, micro-optical structures have been successfully fabricated by using the Sn grayscale masks.

2. Experiments

Tin thin films (thickness 10~50 nm) were deposited on glass substrates (thickness of 0.17 mm) by radio-frequency magnetron sputtering (ULVAC ACS400-C4). A home-built laser direct writer adopted a 532 nm laser (Spectra Physics, Millennia Pro 2i) was applied to write patterns onto the films by raster-scan, the typical scan speed is 50 $\mu m \cdot s^{-1}$, with a scan width of 200 nm smaller than the spot size (~350 nm) and with a repetition rate of 250 Hz. The scan adopts the single pulse exposure with a pulse width of 1 ms and powers ranging from 0 to 8 mW (corresponding energy density 0-80 $J \cdot mm^{-2}$) controlled by an acousto-optic modulator. In the process of mask fabrication, the film sample was firstly placed in an X-Y-Z sample stage (PI, precision 2 nm) at the focal plane of the objective lens (Nikon, NA 0.90, 100 ×), then the grayscale pattern was fabricated according to a 10-bit bitmap file transferred from a color or grayscale picture.

The optical micrographics on the masks were taken using an Olympus BX-51 microscope. The crystal structure evolution of the mask was analyzed by using bright field transmission electron microscopy (TEM), high resolution (HR) TEM and selected area electron diffraction (SAED) measurements (FEI Tecnai G^2 20 ST). Photolithography experiments were carried out with a lithography machine (SUSS MicroTec).

3. Results and discussions

3.1 Laser direct writing of grayscale patterns

The Sn films are found to turn transparent under pulsed-laser exposure and the transparency is dependent on laser power, that is, higher laser power yields larger *T*. Figure 1 shows a set of grayscale patterns with continuous-tone and discrete gray levels fabricated in tin thin film by using LDW technique, displaying good grayscale feature. These patterns can be used as grayscale masks for fabricating typical micro-optical elements. Some complex arbitrarily-shaped grayscale patterns were also successfully obtained.

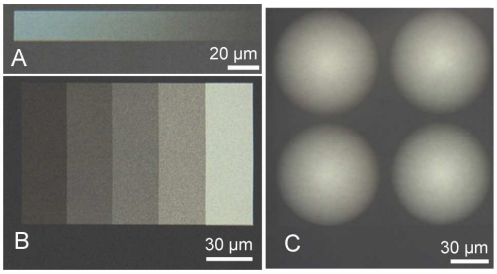

Fig. 1. Optical microscopy (OM) images of a set of typical grayscale masks.

3.2 Mechanism of the grayscale feature

To further understand the nature of the good grayscale feature, the phase evolution in the film was investigated. A 20 nm-thick tin thin film was deposited on a carbon membrane supported by a TEM copper grid and then raster-scanned to make a continuous-tone grayscale bar by a 532 nm laser with the power range of 0-1.0 mW (the power is lower than that on the Sn/glass system because of the much lower thermal-conductivity of carbon membrane) and a pulse width of 1 ms, and the corresponding energy density range is 0-10 $J \cdot mm^{-2}$. Laser power is adopted as the controlling parameter in this paper because it is technically convenient. The film was found to turn transparent at a threshold power of ~0.20 mW, as shown in Fig. 2a. Selected area electron diffraction (SAED) was operated for structural analysis with the selected area diaphragm centered at different areas, which are exposed under various laser

#117173 - $15.00 USD Received 18 Sep 2009; revised 10 Oct 2009; accepted 10 Oct 2009; published 19 Oct 2009

powers of 0.20, 0.30, 0.45, 0.55 and 0.80 mW, respectively. The corresponding SAED patterns indicate that Sn first transform to t-SnO (<0.45 mW), and then to o-SnO_2 and t-SnO_2 (>0.45 mW). At high power region (>0.5 mW) we find small amount of metallic Sn, which has already disappeared at 0.45 mW, this can be interpreted by a well-known reaction defined as:

$$2SnO(t) \longrightarrow Sn + SnO_2(t) \qquad (1)$$

Equation (1) shows the SnO is an important intermediate oxide in the tin/tin oxides system. F. J. Lamelas *et al*. proposed SnO is a requisite for the formation of o-SnO_2 [22]. The t-SnO_2 is originated from two ways: decomposition of SnO according to Eq. (1) and oxidation of o-SnO_2 at high temperatures. Our further study shows that as laser power increases to higher than 0.8 mW, the amount of both Sn and o-SnO_2 gradually reduces and leads to even higher transparency. The SAED patterns also show mixture nature of the laser exposed areas. The structural analysis clearly indicates that the continuous-tone grayscale feature originates from the phase evolution and coexistence of different phases.

Beside the above mentioned phases, transparent amorphous SnO_x (a-SnO_x) was found at low powers and it also plays a very important role. From Fig. 2(b) and (c) one can learn that the amount of Sn is reduced after laser exposure according to the reduction of diffraction intensity. This is because Sn grains are coated with a layer of a-SnO_x (see the HRTEM image in Fig. 3(a)), and its thickness increases (or volume of Sn decreases) after laser exposure. The a-SnO_x is the precursor of SnO and subsequent tin oxides: SnO was found to nucleate and grow in the amorphous layer at above 0.3 mW (see Fig. 3(b)), and the film has almost transformed to SnO completely at ~0.45 mW.

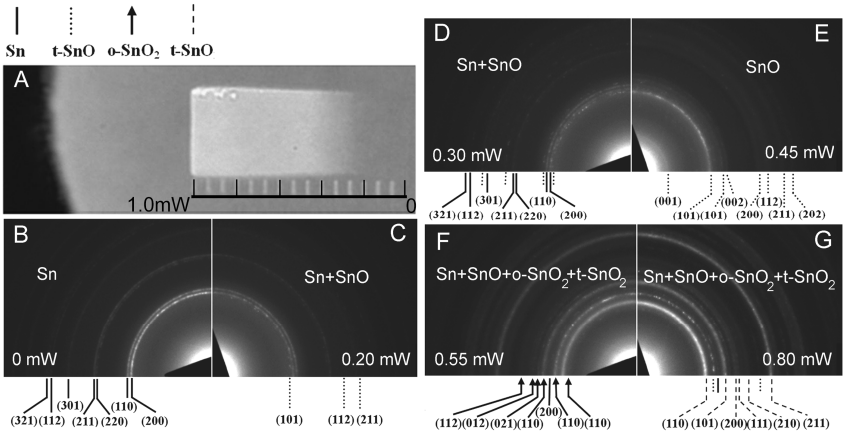

Fig. 2. (a) A grayscale bar on carbon membrane; (b)-(g) SAED patterns at different laser powers, showing the phase evolution dependence on laser powers.

In an amorphous SnO_x coat there is always several SnO nuclei (Fig. 3(b)), as they grow up, an as-deposited Sn grain turns to several SnO subgrains or subsequent SnO_2 subgrains with a diameter of ~5 nm, two orders smaller that the wavelength of visible light. The nanoscale fine Sn grains (~20 nm) are crucial in this system because larger grains (submicro-scale) cannot be completely oxidized and will result in non-uniform in both morphology and transmittance. At powers over 0.45 mW, SnO decompose to Sn (which can be easily oxidized) and t-SnO_2 in a disproportionation reaction, or is further oxidized to o-SnO_2. The t-SnO_2 is the major product. HRTEM images also confirm the phase evolution and coexistence of the oxides (Fig. 3), and that's why the patterns possess continuous-tone grayscale feature. The phase evolution in the films is very complicated, how does the nanocrystalline affect transparency quantitatively still need further study. Fortunately, experimental results have

#117173 - $15.00 USD Received 18 Sep 2009; revised 10 Oct 2009; accepted 10 Oct 2009; published 19 Oct 2009

shown that the transparency can be well controlled so that the Sn films can be used as grayscale masks practically.

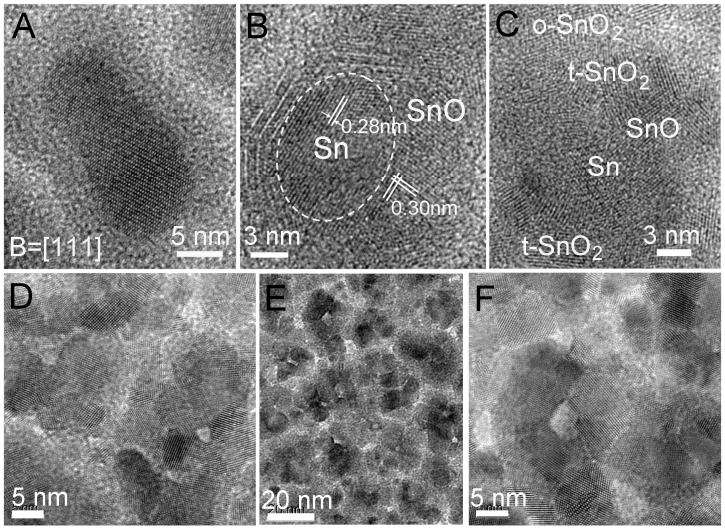

Fig. 3. Structural and amorphous evolution of Sn films under various laser powers. HRTEM images of: (a) 0 mW, (b) 0.4 mW, (c) 0.5 mW, (d) 0.6 mW and (f) 0.8 mW. (e) Bright-field TEM image of 0.8 mW laser exposed Sn film, showing grains composed of several sub-grains.

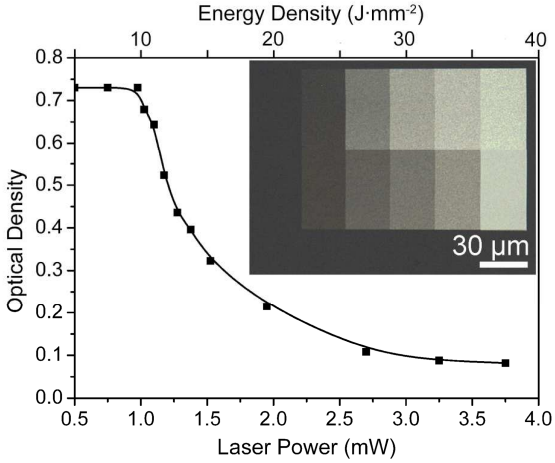

Fig. 4. OD versus laser power with a pulse width of 1 ms. The inset is five-level grayscale bars before (the upper) and after grayscale calibration (the bottom) using the OD-laser power curve.

3.3 Grayscale calibration and fabrication of 3D microstructures

The transparency of the films is the most important since the films are aimed at grayscale masks. The optical density (OD = –lg*T*) of a 20 nm thick film is found to change from 0.73 OD to 0.08 OD at 532 nm (*T* from 19% to 83%, and the corresponding laser power from 0.9 to 3.6 mW and energy density of laser spot from 9 to 36 J·mm^{-2}) after laser irradiation, shown in Fig. 4. The nonlinear relationship of laser power and optical density should be calibrated for designing specific curved surfaces. In Fig. 4, a grayscale bar (laser power or energy density is linearly increased along X direction) with unfavorable gray levels was improved by correction of nonlinearity using the OD-laser power curve. The grayscale calibration is able

#117173 - $15.00 USD Received 18 Sep 2009; revised 10 Oct 2009; accepted 10 Oct 2009; published 19 Oct 2009

to design various masks for 3D microstructures with specific profiles. Based on this, we can make 3D microstructures as we designed.

For further examining the practical applications of the Sn grayscale masks, gray-tone lithography was done. In the primary photolithography experiments, some 3D microstructures with specific curved surface, for example, micro-lens arrays, micro-taper *etc*. have been made on photoresist (Fig. 5), by using Sn grayscale masks photolithography. This indicates the novel grayscale mask can actually work.

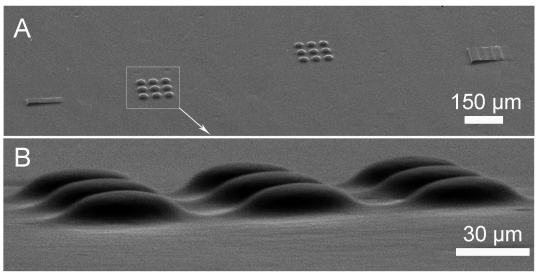

Fig. 5. 3D microstructures fabricated in SU-8 photoresist: (a) 60° and (b) 85° tilt-view images.

3.4 Stability of the Sn grayscale masks

Since a grayscale photomask is obtained through a pulsed-laser-induced thermal oxidation process, its stability to light and heat is rather important. It is well known tin is a stable metal at room temperature so that it is often used as a protective layer on iron. The high stability of the tin thin film may be related to the amorphous SnO_x layer that has been verified by TEM [20]. Also all the tin oxides involved in are stable in the form of film under ambient conditions [19,22]. In order to confirm the photothermal stability of the Sn grayscale mask experimentally, a film with grayscale patterns was firstly placed under a 40 W bulb irradiation at a distance of 5 cm for 2 h and then heated at 100°C temperature for 2 h, the results showed no obvious change and indicated its good photothermal stability.

Conclusions

In summary, we used laser direct writing to make grayscale masks in very simple media: Sn nano-films. The Sn grayscale masks demonstrate excellent properties in various aspects of continuous-tone gray levels, simple fabricating techniques, low cost and good stability. The mechanism of the grayscale feature is proposed: the film undergoes various oxidation processes with a typical phase transformation sequence of Sn $\rightarrow$ SnO$\rightarrow$ (o- and t-) SnO_2 with the increasing of laser powers. Phase evolution observed by SAED and HRTEM shows mixture nature in the exposed area when the laser power exceeds a conversion threshold. Among these oxides, the phases formed at high powers (t- and o-SnO_2) are more transparent than that at low powers (SnO and Sn). As a result, the transmittance (grayscale) can be well controlled by simply adjusting the laser power (or the energy density), thus the fabrication of grayscale masks is extremely simple by using LDW technique. Our study reveals that the grayscale feature of the film roots in 1) transmittance differences of different phases and 2) the coexistence of multi-phases in various components. The nanoscale fine grains of the film are crucial for the controllable transparency. 3D microstructures with specific curved surface have been successfully made using the novel grayscale masks. Our results show that Sn thin film is a promising material for fabricating grayscale masks because it possesses merits of both HEBS glass and COG grayscale masks while absents their disadvantages.

To be clarified, Sn is not the sole metal to have grayscale feature, other metals such as In, Al and Zn which have transparent oxides can also be used as potential grayscale materials. Therefore, this technique enables the fabrication of low cost grayscale masks for 3D lithography and provides a new opportunity in the fields of mechanical, optical and electronic applications.

#117173 - $15.00 USD Received 18 Sep 2009; revised 10 Oct 2009; accepted 10 Oct 2009; published 19 Oct 2009

Acknowledgement

This work was partly supported by the 863 program (2006AA03Z353), NSFC (90606025), the KIP of CAS (KJCX2-YW-M06) and NBRPC (2010CB934102).

#117173 - $15.00 USD Received 18 Sep 2009; revised 10 Oct 2009; accepted 10 Oct 2009; published 19 Oct 2009